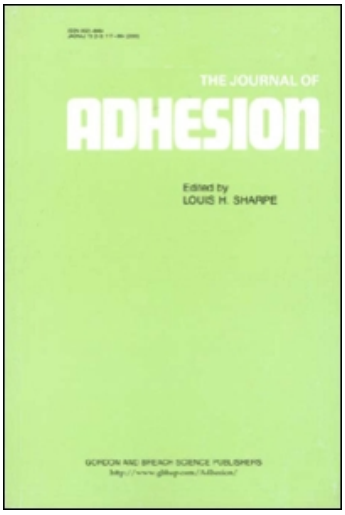

The Journal of Adhesion

Publication details, including instructions for authors and subscription information:
http://www.informaworld.com/smpp/title~content=t713453635

Stresses between Adherends with Different Curvatures

David A. Dillard[a]
[a] Engineering Science and Mechanics Department, Virginia Polytechnic Institute, Blacksburg, Virginia, U.S.A.

To cite this Article Dillard, David A.(1988) 'Stresses between Adherends with Different Curvatures', The Journal of Adhesion, 26: 1, 59 — 69
To link to this Article: DOI: 10.1080/00218468808071274
URL: http://dx.doi.org/10.1080/00218468808071274

J. Adhesion, 1988, Vol. 26, pp. 59–69
Reprints available directly from the publisher
Photocopying permitted by license only

Printed in the United Kingdom

Stresses between Adherends with Different Curvatures

DAVID A. DILLARD

Engineering Science and Mechanics Department, Virginia Polytechnic Institute, Blacksburg, Virginia 24061, U.S.A.

(Received December 24, 1987; in final form April 2, 1988)

Closed form solutions are derived to predict the peel stresses developed between adherends which form a parallel bond but would have slightly different curvatures in their unbonded, stress-free states. The solutions are based on beam on elastic foundation analysis and may be applicable to a variety of geometries. Failure analysis based on a maximum stress criterion as well as a fracture mechanics approach are also provided. The possibility of using the analysis as the basis for a fracture test is also discussed.

KEY WORDS Winkler foundation; beam on elastic foundation; adhesive stresses; curved adherends; failure analysis; residual stresses.

INTRODUCTION

Most adhesive joints are designed to resist some externally applied mechanical loading, although occasionally thermal expansion or other factors can induce significant residual stresses in an otherwise unloaded joint. This paper addresses the residual peel stresses within an adhesive layer which result from forcing together and bonding adherends with slightly different initial curvatures. Typical geometries might include bonding flat strips or plates to curved surfaces, curved strips to flat surfaces or, in general, bonding together any two cylindrically curved plates with parallel axes but different curvatures. This analysis originally arose out of an attempt to understand why the author's warped nameplate partially de-

bonded from his door over time, but has direct applicability to a variety of serious adhesive problems including the debonding of molding strips from automobiles. The difference in stress-free curvature may arise from an initial mismatch prior to bonding, or it may result from temperature or moisture gradients, from thermally induced curvature in nonhomogeneous adherends, or from a difference in solvent content across one of the adherends as could arise from drying or solvent outgassing over extended periods of time.

The analysis may also have bearing on stresses which occur in paints or coatings, as well as stresses which occur between the thin layers in microelectronic chips. The applicability to these situations is not complete, however, because the analysis assumes a distinct adhesive layer exists with a lower modulus than the adherends. Furthermore, in the case of coatings, the high peel stresses primarily arise from differences in thermal expansion between the film and the substrate. This in-plane stretching effect has not been considered in this paper which is limited to the peel stresses arising from a curvature mismatch. Techniques to evaluate strain energy release rates for this stretching mode have been presented elsewhere.[1] For linear systems, the solutions may be easily superimposed, although for very thin adherends such as films, the membrane stiffness is so much greater than the bending stiffness that the curvature effect may be negligible.

FORMULATION OF ANALYSIS TECHNIQUE

Several potential geometries may be addressed with the solution. Figure 1 illustrates several cases of interest with either positive or negative curvatures of a rigid substrate and a flexible adherend. Figure 2 shows a case with two flexible adherends which is also easily analyzed by the technique discussed herein. For convenience, we develop our model around the geometry shown in Figure 3 where an initially curved strip is forced into contact with a flat, rigid substrate. The bending stiffness of the flexible member is constant and is given by EI, where E is the modulus and I is the moment of inertia of the cross-section. The modulus of the adhesive is E_a, the nominal thickness of the adhesive layer is h and the width of the

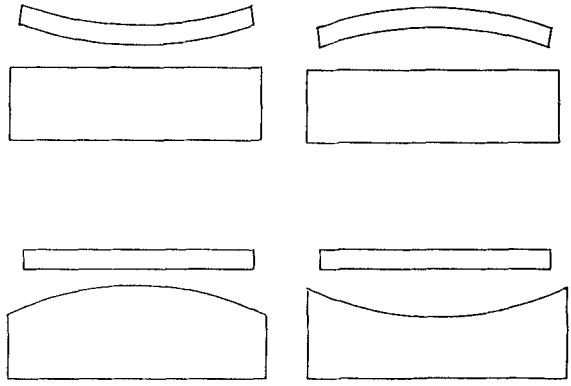

FIGURE 1 Typical configurations of a flexible adherend and a rigid substrate.

adhesive strip is w. The bonded length of the beam is $2L$, but L decreases as debonding occurs. Curvatures are considered positive if the surface is concave up. The shear and bending moment conventions are also shown in Figure 3. Although the derivation is based on a beam geometry (plane stress), the solution may easily be extended to a plate configuration (plane strain) by replacing EI/w with D, the plate bending stiffness, and E_a with $E_a(1-\nu_a^2)$, where ν_a is the Poisson's ratio of the adhesive. For plates on elastomeric

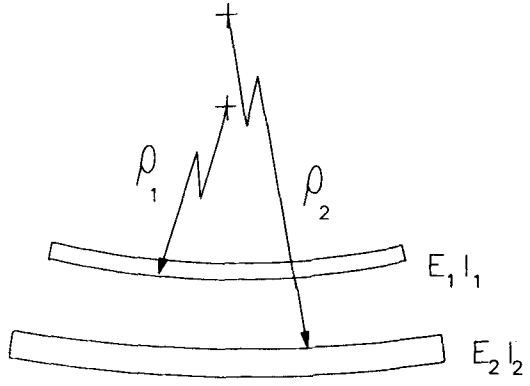

FIGURE 2 General configuration with both adherends flexible and initially curved.

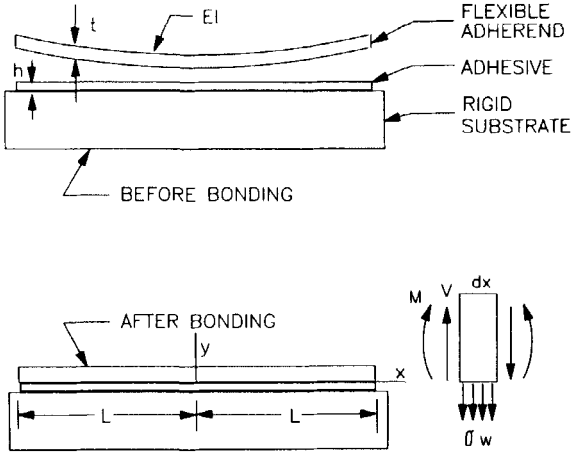

FIGURE 3 Sign conventions and dimensions for the analysis.

adhesives, alternate governing equations discussed in Ref. 2 should be used.

The solution technique is based on a beam on elastic foundation analysis attributed to Winkler and discussed in detail by Hetényi.[3] To satisfy the necessary assumptions, we will require that the curvatures of the adherends be small in comparison to the thickness of the flexible adherend so standard beam theory will apply, that the modulus of the adherends be large compared to that of the adhesive so strains perpendicular to the bond plane be negligible in the adherends, and that the length of the adherend is at least an order of magnitude greater than the thickness of the adherend in order to be able to neglect shear deformations in the adherends. The requirement that the curvature be small does not preclude the use of this technique from geometries with large subtended angles, but simply requires that t/ρ be small, where ρ is the radius of curvature, and t is the nominal thickness of the beam.

For convenience, the derivation is given for the case of one flexible adherend bonded to a rigid substrate, although extension to the case of two flexible beams as shown in Figure 2 may be easily addressed as follows. If the two beams have stiffnesses of E_1I_1 and E_2I_2, respectively, the effective beam stiffness becomes the inverse

of the sum of the individual compliances:

$$EI = \frac{E_1 I_1 E_2 I_2}{E_1 I_1 + E_2 I_2} \tag{1}$$

If both adherends are curved, we may use the net curvature:

$$\frac{1}{\rho} = \frac{1}{\rho_1} - \frac{1}{\rho_2} \tag{2}$$

The curvatures are always measured at the bond surface of the adherend. Since the flexible adherend thickness is small compared with the curvature, we can use this value of bond surface curvature rather than the curvature of the neutral axis without appreciable error in the beam equations.

Considering a differential element from the beam, we recognize that expressions for the shearing force, V, and bending moment, M, are given by:

$$\frac{dV(x)}{dx} = -\sigma(x)w \tag{3a}$$

$$\frac{dM(x)}{dx} = V(x) \tag{3b}$$

where $\sigma(x)$ is the peel stress in the adhesive. If we assume that the adhesive is linear elastic, we may write that:

$$\sigma(x) = \frac{E_a}{h} y(x) \tag{4}$$

where y is the deflection of the beam.

Assuming that the slopes are small (which is a good assumption over any localized region), we can use simple beam theory to write:

$$\frac{d^2(y - y_0)}{dx^2} = \frac{M}{EI} \tag{5}$$

where y_0 is the stress-free shape of the adherend given by:

$$y_0(x) = \frac{x^2}{2\rho} \tag{6}$$

(We assume that the initial curvature is constant and over any small section is adequately modeled by this parabolic form.)

Differentiating twice and substituting in Eqs. (3a) and (3b), we obtain

$$\frac{d^4y}{dx^4} + 4\lambda^4 y = 0 \tag{7}$$

where

$$\lambda = \left(\frac{E_a w}{4EIh}\right)^{1/4} \tag{8}$$

and recognize that this is simply the equation for a beam on an elastic foundation with a solution given by:

$$y(x) = e^{-\lambda x}(A \cos \lambda x + B \sin \lambda x) + e^{\lambda x}(C \cos \lambda x + D \sin \lambda x) \tag{9}$$

subject to the boundary conditions at the ends:

$$M(-L) = M(L) = V(-L) = V(L) = 0$$

Details for this derivation can be found in any good advanced mechanics of materials text, such as Ref. 4.

We now proceed to solve this equation for our particular boundary conditions and loading function. By symmetry, we recognize that $A = C$ and $B = -D$. We make use of one bending moment and one shear force boundary condition and obtain that:

$$A = C = \frac{-\cosh \lambda L \sin \lambda L + \sinh \lambda L \cos \lambda L}{2\rho\lambda^2(\sinh 2\lambda L + \sin 2\lambda L)} \tag{10}$$

and

$$B = -D = -\frac{\cosh \lambda L \sin \lambda L + \sinh \lambda L \cos \lambda L}{2\rho\lambda^2(\sinh 2\lambda L + \sin 2\lambda L)} \tag{11}$$

Figure 4 illustrates the beam deflections as a function of position for several beam lengths. As might be expected, we note that for beam lengths greater than $4/\lambda$, the deflection is relatively unchanged in the vicinity of the beam end and is nearly zero at all intermediate points within the beam. By evaluating the deflection at the end of the beam, we obtain

$$y(L) = \frac{1}{2\lambda^2\rho}\left(\frac{\sinh 2\lambda L - \sin 2\lambda L}{\sinh 2\lambda L + \sin 2\lambda L}\right) \tag{12}$$

which for large λL becomes

$$y(L) \approx \frac{1}{2\rho\lambda^2} \quad \text{for } \lambda L > 4, \tag{13}$$

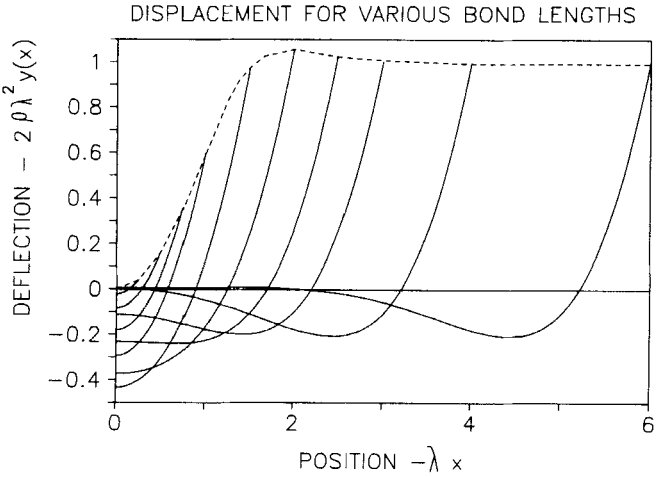

FIGURE 4 Deflected shape of various beam lengths.

and for very small λL is

$$y(L) \approx L^2/3\rho \quad \text{for } \lambda L < 0.5$$

At intermediate values, we observe from Figure 4 that the tip deflection reaches a maximum value of $\sim 1.057/(2\rho\lambda^2)$ near $\lambda L = 1.95$. For values of $\lambda L < \sim 1.5$, the tip deflection drops below that for long bonds.

By making use of Eq. 4, Figure 5 shows the details of the peel

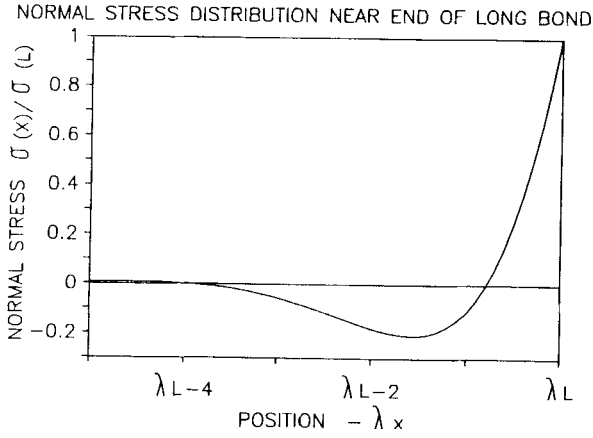

FIGURE 5 Normal stress distribution near the end of a long beam.

stress distribution at the end of a sufficiently long joint. The net force acting perpendicular to the beam is zero, and the moment generated by the stress distribution is just that required to offset the curvature.

FAILURE ANALYSIS WITH POSITIVE CURVATURE MISMATCH

To develop an appreciation for debonding of the joint, we now proceed using the peel stress as given by Eq. 4. For the preceding analysis to remain valid, we will assume that the adhesive is linear elastic up to failure. If we use a simple maximum stress failure criterion, we gain insights into the failure process although, admittedly, we have neglected any singularities associated with the flaw tip or the material property mismatch.[5] Starting the analysis for long beams by setting the failure strength, σ_f equal to $\sigma(L)$:

$$\sigma_f = \sigma(L) = y(L)\frac{E_a}{h} = \frac{E_a}{2\rho\lambda^2 h}, \tag{14}$$

we require that the curvature must not exceed

$$\frac{1}{\rho} \leq \frac{2\sigma_f \lambda^2 h}{E_a} \tag{15}$$

in order to avoid failure. For values of curvature greater than this, we observe from Figure 4 that debonding would be expected to occur until the maximum stress is reduced once λL falls below ~1.5. Use of Eqs. 12 and 4 would permit calculation of the final size of the bonded region. This prediction corresponds well with experimental observations that debonding occurs only a certain distance from each end, leaving a central region which is bonded and stable.

If a fracture mechanics criterion is used to investigate debonding for the case of a long bond length, a very simple expression results. As long as λL is greater than 4, we notice that an increment in debond does not alter the shape of the deflected beam near the tip, but simply shortens the total length. A significant observation is that even the stresses in the adhesive remain unchanged; they are simply shifted in position. In essence, the only stored strain energy which

drives the debond is the energy which would come from an equivalent length increment at the center of the beam. Since the adhesive strain energy is zero away from the tip region, we conclude that the only available strain energy must come from the bending energy in the beam required to produce the nominal curvature, ρ. Considering the applicable energy balance equation

$$-\delta U = G\delta A$$

and the energy in a beam subjected to a fixed curvature

$$\delta U = \frac{M^2}{2EI}\delta x = \frac{EI}{2\rho^2}\delta x$$

we obtain the available strain energy release rate as:

$$G = \frac{EI}{2w\rho^2} \tag{16}$$

where ρ is defined as in Eq. 2. Interestingly, no restrictions are placed on the thickness or flexibility of the adhesive layer because the stored energy in the adhesive remains unchanged for long bond lengths.

FAILURE ANALYSIS WITH NEGATIVE CURVATURE MISMATCH

Another important configuration is when the initial curvature is negative. The peel stress distribution is simply reversed in sign, and we recognize that compressive stresses normal to the bond plane will result at the ends of the beam. The maximum positive deflection will occur at distances $\pi/2\lambda$ inward from the ends. The first location of zero displacement occurs a distance of $\pi/4\lambda$ inward from the ends. The magnitude of the displacement at the $\pi/2\lambda$ location is given by

$$y\left(L - \frac{\pi}{2\lambda}\right) = \frac{-1}{2\rho\lambda^2}\frac{1}{\cosh \pi/2 + \sinh \pi/2} \approx 0.2079\left(\frac{-1}{2\rho\lambda^2}\right) \tag{17}$$

or about one-fifth of the maximum deflection at the tip.

Again, one may apply an appropriate failure criterion to identify the critical value of negative curvature for failure. Assuming that

the critical position is where the tensile stress is highest and using a maximum stress criterion, we note that

$$-\frac{1}{\rho} \leq 9.62\sigma_f \lambda^2 h/E_a \tag{18}$$

For shorter bond lengths, we note from Figure 4 that significantly larger values of the maximum deflection occur than predicted by Eq. (17). The largest deflection occurs when $\lambda L = \pi/2$ and is equal to $-0.4345/(2\rho\lambda^2)$ representing a 109% increase over Eq. (17).

It should be noted that for the case of negative curvature the analysis, once partial debonding occurs, is complicated by the fact that the debonded region is forced back on the substrate, inducing an additional moment on the flexible adherend. This has not been addressed in this analysis. The use of a fracture criterion also becomes more involved because tensile stresses are not carried at the debonded region, thereby causing the governing equation to be invalid. A numerical solution to this problem could be used to address these aspects.

CONCLUSIONS

Simple, closed-form expressions have been derived for predicting the peel stresses which result between beams or plates with a mismatch of curvature. The results clearly show why such configurations may debond over long distances. Both positive and negative curvature mismatches have been considered.

Failure criteria based on maximum stress and a fracture mechanics approach for these joints have been discussed. This joint geometry produces a very constant strain energy release rate fracture mode which could conceivably be used for a fracture test. Since the specimen is self-loading, however, the strain energy release rate could not be changed conveniently once a given specimen geometry has been fabricated. Such a technique could be adapted to measure the debonding rate for environmentally-exposed specimens. Since the available strain energy does decrease as the debonding fronts approach each other, the test could also measure a threshold value of fracture toughness. By changing the

radius of curvature of the substrate, varying values of strain energy release rate could be achieved with the same specimen.

Acknowledgements

The author would like to acknowledge the technical encouragement and support received through Dr. J. Scott Thornton, Texas Research Institute, Austin, Texas, U.S.A. Special thanks are also given to Shelia Lucas for typing the manuscript.

References

1. S. G. Croll, in *Adhesion Aspects of Polymeric Coatings,* K. L. Mittal, Ed. (Plenum Press, New York, 1983).
2. D. A. Dillard, *Journal of Applied Mechanics,* in review.
3. M. Hetényi, *Beams on Elastic Foundations* (University of Michigan Press, 1946).
4. F. B. Seely and J. O. Smith, *Advanced Mechanics of Materials* (2nd. Edition Wiley New York, 1952).
5. G. P. Anderson, S. J. Bennett, and K. L. DeVries, *Analysis and Testing of Adhesive Bonds,* (Academic Press, New York, 1977).